THE RNA AND PROTEINS OF HUMAN CORONAVIRUSES

John C. Hierholzer, Maurice C. Kemp, and
Gregory A. Tannock*

Respiratory Virology Branch, Virology Division, Center for Disease Control, Atlanta, Georgia, U.S.A. 30333; and *G.A.T.: Division of Clinical Investigation, Faculty of Medicine, University of Newcastle, New South Wales 2308, Australia

Coronaviruses were classified as a distinct group of viruses in 1968[1] and are now recognized as the etiologic agents of an increasing number of diseases of man and animals[2-7]. At least four members of the group are human respiratory pathogens. Others have been suggested to be involved in neurologic and enteric disease processes in man, although none of these strains have yet been isolated in the true sense of the word.[8-18] Respiratory strain B814 was the first human coronavirus discovered, having been isolated in human embryonic tracheal organ culture by Tyrrell & Bynoe in 1960.[19] Strain 229E was recovered in secondary human fetal kidney cell cultures by Hamre & Procknow in 1962.[20] Strain OC-43 and many related strains were then found by organ culture techniques in 1966 by McIntosh et al.[21] Strain 692 was identified by immune electron microscopy in 1966 by Kapikian et al.[22]

None of these strains are readily adaptable to laboratory procedures. They replicate poorly if at all in conventional cell cultures; they tend to be highly labile under conditions of virus purification; and they do not produce soluble antigens which can be measured by routinely available serologic tests. For these reasons, detailed analyses of the protein and nucleic acid structure of the respiratory coronaviruses have not kept pace with similar studies on avian and mammalian coronaviruses.

Despite the difficulties, much has been learned about the structure of two of the human respiratory coronaviruses in the past 5 years. In this paper, we will review these data to bring the human coronaviruses into perspective with the biochemistry and biology of the other animal coronaviruses.

V. ter Meulen et al. (eds.), *Biochemistry and Biology of Coronaviruses*

BIOLOGICAL ACTIVITY TESTS FOR STRAINS OC-43 AND 229E

The original strains OC-43 and 229E, as well as other isolates of these same "types," have been thoroughly checked for antigenic relatedness to animal coronaviruses by complement-fixation (CF) and immunodiffusion (ID) tests.[23,24] In addition to CF, human infections by both strains are readily detected by indirect fluorescent antibody (IFA) tests on shed respiratory cells and secretions[25] and on acute and convalescent serum specimens.[26] Antibody to both OC-43 and 229E can also be measured by single radial hemolysis (SRH) tests.[27,28]

Strain OC-43, adapted to suckling mouse brain and grown to high infectivity titer, was found to possess a hemagglutinin (HA) for human "O", vervet monkey, chicken, rat, and mouse cells.[29] This HA activity has been essential in virus purification studies as a readily quantifiable marker[30-32] and is useful in documenting human infection by hemagglutination-inhibition (HI) tests on patients' acute and convalescent serum specimens.[26-29,33,34] OC-43 has also been detected in cell cultures by hemadsorption (HAd) tests with rat or mouse cells.[34] A plaque-reduction neutralization test for OC-43 in MA-321 microcultures has been described which appears to be more sensitive than the HI test for measuring human serologic response to infection.[33] Finally, antibody response to OC-43 infection measured by solid-phase radioimmunoassay (RIA) was found to be comparable to that measured by CF, HI, or SRH tests.[35]

Strain 229E is readily identified by serum neutralization (SN) tests in various cell cultures.[23,26,36] In addition, sensitive indirect hemagglutination (IHA) and immune-adherence hemagglutination (IAHA) tests were developed to measure serum antibodies.[36,37] An indirect ELISA test was recently used for 229E but has not yet been applied to human serology.[38]

PROTEINS OF STRAIN OC-43

Utilizing its properties of hemagglutination and high-titered growth in suckling mouse brain, OC-43 was extensively purified by temperature-dependent adsorption to and elution from fresh human "O" erythrocytes and by batch $CaHPO_4$ chromatography.[31] The final purified virus suspension was concentrated by ultrafiltration with XM-300 Diaflo membranes (Amicon Corp.). The virus was purified to a 5000-fold decrease in total protein with a yield of 90% and a final HA titer of 1.3×10^5. The purity of the virus was confirmed by immunologic procedures, density gradient centrifugation, electron microscopy, and analytical procedures.[30] Electron microscopy at low and high magnifications showed very clean fields of particles exhibiting the pleomorphism typical of this virus. Analytical ultracentrifugation revealed a sharp peak at 15,000 rpm with as

little as 1.0 mg protein in the sample; this peak had the same sedimentation rate as one of several broad peaks observed when crude virus (at 2-4 mg protein/.4 ml) was sedimented under identical conditions. Acrylamide gels loaded with untreated concentrated supernatant fluids obtained from centrifugation (23,800g, 2 hr) of purified virus suspensions revealed no protein bands.[30]

Mouse ascitic fluid and mouse antiserum prepared against crude virus and against purified virus gave predominantly single bands (of identity) with pure or crude virus in standard ID tests. However, tests with guinea pig and chicken anti-crude and anti-pure virus sera showed two precipitin bands of complete identity between pure and crude virus, and one additional band of identity between pure virus, crude virus, and normal mouse brain. These results suggest that the OC-43 virion contains at least one mouse-brain antigen. Additional evidence of host antigen in the intact virion was found by an identical line between anti-normal mouse-brain serum and the three concentrated antigens. Immunoelectrophoresis of these same antigen-antiserum combinations demonstrated three or four precipitin arcs with crude virus and two or three arcs with purified virus, and confirmed the presence of a mouse-brain protein associated with the purified virus.[30]

The virus was solubilized with SDS/mercaptoethanol/urea, and the resulting polypeptides were separated by PAGE. The staining patterns with Coomassie blue revealed a minimum of six bands, five of which might be considered major. One additional faint band was occasionally observed between the top two bands.[30]

The molecular weights of the viral proteins were determined by co- and companion electrophoresis with proteins of known molecular weight (Table 1). Gels were also stained for lipid and carbohydrate. The lipid content of the single lipoglycopolypeptide was more evident in gels in which the sample was not heated than in those in which it was heated at 100°C for 1 min. However, the classification of the polypeptides as glyco- or lipoglycoproteins must be considered as only tentative, since the chemical nature of these complexes cannot be precisely defined by differential staining techniques. The use of more sensitive procedures to confirm the nature of these proteins awaits the successful adaptation of OC-43 to high-titered growth in cell cultures.

The peplomers on the virion surface have previously been associated with HA activity and are thought to comprise the major antigens measured by both the HI and CF tests. Hence the envelope-associated antigens, unlike influenza virus, appear to consist of a single species. Absence of neuraminidase was confirmed using highly sensitive assay systems. Attempts to determine directly which polypeptides comprise the external antigen, by eluting bands from acrylamide gels in PBS, dialyzing, and titrating for direct and

Table 1. Polypeptides of Strains OC-43 and 229E

Virus	Polypeptide number[a]	Approx. MW (mean)	% comp. (mean)	Probable function/location	Reference
OC-43	VLGP-191	191,200	13	peplomer dimer	Hierholzer et al (1972)[30]
	VP-165	165,000	2	peplomer base	
	VGP-104	104,000	8	peplomer monomer	
	VGP-60	59,500	22	double-shelled envelope	
	VP-47	47,100	16	core (RNA-associated)	
	VP-30	30,500	25	double-shelled envelope	
	VGP-15	15,000	14	peplomer	
229E	VLGP-196	196,100	15	peplomer dimer	Hierholzer (1976)[40]
	VGP-165	165,000	3	peplomer base	
	VGP-106	105,500	8	peplomer monomer	
	VGP-66	65,500	21	double-shelled envelope	
	VP-47	47,300	16	core (RNA-associated)	
	VGP-31	31,400	20	double-shelled envelope	
	VGP-17	16,900	17	peplomer	
229E	VGP-160	160,000	ND	surface projections	Macnaughton (1980)[42]
	VGP-105	105,000	ND	surface projections	
	VP-50	50,000	ND	internal component	
	VGP-24	24,000	ND	?	
	VP-22	22,000	ND	?	

[a]Designated as V=viral, L=lipo, G=glyco, P=protein

indirect hemagglutination, were unsuccessful because residual SDS adversely affected the erythrocytes. Repeated attempts to determine the composition of the external antigen by selectively removing the entire peplomer from the virus envelope also were of limited value. So, membrane-associated components were identified indirectly by bromelin digestion in a reducing buffer with dithiothreitol. The effect of bromelin treatment on purified virus was monitored every 30 minutes under the electron microscope. The club-shaped projections were completely degraded after 2 hours of incubation at 37°C with 0.13% bromelin. The 2-hour test samples, along with the appropriate virus and enzyme controls, were repurified on 5-40% aqueous neutral potassium tartrate gradients at 75,000g for 8 hr. The untreated control virus banded in the 1.18 g/cm^3 region of the gradient and was associated with a sharp HA peak; by EM this band consisted of typical virions. The bromelin-treated virus banded in the 1.15 g/cm^3 region of the gradient; by EM this band contained fully enveloped virions which lacked surface projections. All biological activity was lost by the enzyme treatment (Table 2). Polypeptides of the repurified virion control and of the bromelin-treated virions were analyzed by SDS-PAGE. Two major polypeptides, both glycoproteins, and the minor VP-165 were absent in the bromelin-treated sample. However, exactly which proteins comprise the peplomers remains to be confirmed, because the molecular weight

Table 2. Properties of Bromelin-treated OC-43 Virus

Sample[a]	Buoy. dens. (g/cm^3)	Infectivity ($log_{10}LD_{50}$/ 0.02 ml, SMB)	Antigen titer[b] HA	CF	No. bands in PAGE	No. of preci. arcs in IE
1 Control virus	1.18	9.8	32,768	128	7	3
2 Bromelin-treated v.	1.15	0.7	<1	<2	4	1
3 Bromelin control	--	0.0	<1	<2	0	0

[a]Harvests from potassium tartrate gradients after equilibrium centrifugation at 75,000 g for 8 hr: No. 1 was purified virus incubated for 2 hr at 37°C with 0.1 M Tris-HCl buffer, pH 7.2, containing 0.001 M EDTA and 0.005 M DTT (final concentration), and collected from the 1.18-1.19 g/cm^3 region of the gradient; No. 2 was purified virus treated with 0.13% bromelin in the above buffer at the same conditions, and collected from 1.15-1.16 g/cm^3 region of the gradient; No. 3 was the equivalent amount of bromelin and buffered medium incubated with PBS and collected from a gradient in a manner identical to sample No. 2.

[b]Titers expressed as reciprocals of the endpoint dilution.

estimates of proteins by acrylamide gels are often highly inaccurate at both the high and the low ends of the standard curve. In fact, we suspect that the MW estimate of VGP-104 is probably high under the gel systems used, and that VGP-104 might really be the monomeric form of VLGP-191. This is currently being investigated by more precise methods.

Analytical ultracentrifugation of intact, purified virus (HA titer = 2.6×10^5) at 15, 16, and 18,000 rpm revealed a single distinct peak with a sedimentation coefficient ($s_{20,b}$) of $368 \pm 14 \times 10^{-13}$ sec. Corrections for physical/chemical parameters and for virus concentration gave a fully corrected sedimentation coefficient ($S^{\circ}_{20,w}$) of 390 ± 16 S. The apparent molecular weight was then calculated to be $112 \pm 5 \times 10^6$ daltons, so that the particle weight of one OC-43 virion is approximately $18 \pm 1 \times 10^{-17}$ g.[30]

Our data, therefore, indicate that the HA, CF, and infectious virus activities of OC-43 are associated with the peplomers, and that the intact virion has a density of 1.18 g/cm^3 and a sedimentation coefficient of approximately 390 S.[30] Other workers have reported somewhat different data. Pokorny et al. found the maximum CF activity of OC-43 in sucrose gradients to be in the ribosomal region of 1.14 g/cm^3, HA activity and intact virus to be in the microsomal fraction (1.16 g/cm^3), and incomplete or damaged particles to be in the mitochondrial fraction (1.19 g/cm^3).[32] Sheboldov et al. reported that the density of OC-43 virus in CsCl gradients was 1.24 g/cm^3 and of OC-43 ribonucleoprotein was 1.31 g/cm^3.[39] From sucrose gradient centrifugation data, they found the sedimentation coefficient of the virion to be 280 S and that of the RNP to be 180 S.[39] However, calculation of sedimentation coefficients by this procedure is very approximate, as none of the controls or physical correction factors can be applied.

PROTEINS OF STRAIN 229E

As a prerequisite for studying the polypeptide composition of 229E, it was necessary to closely define its growth parameters in cell culture.[40] Optimum growth was achieved using a medium consisting of Eagles MEM with twice the normal concentrations of amino acids and vitamins and 2% fetal calf serum. Growth characteristics for an MOI of 0.1 and 1.0 are shown in Fig. 1.

Peaks of infectious virus were obtained at 24 hr, with a rapid decline occurring after this time indicating that the virus is highly labile. The growth of infectious virus was paralleled by the extracellular incorporation of labeled amino acids into TCA-precipitable material. Slightly lower titers were obtained for multiplicities of 10.0 and much lower for MOI's of 0.01 and 0.05. When additional vitamins and amino acids were not used, the yield was decreased by 300-fold. Preliminary amino acid analyses on purified virus showed

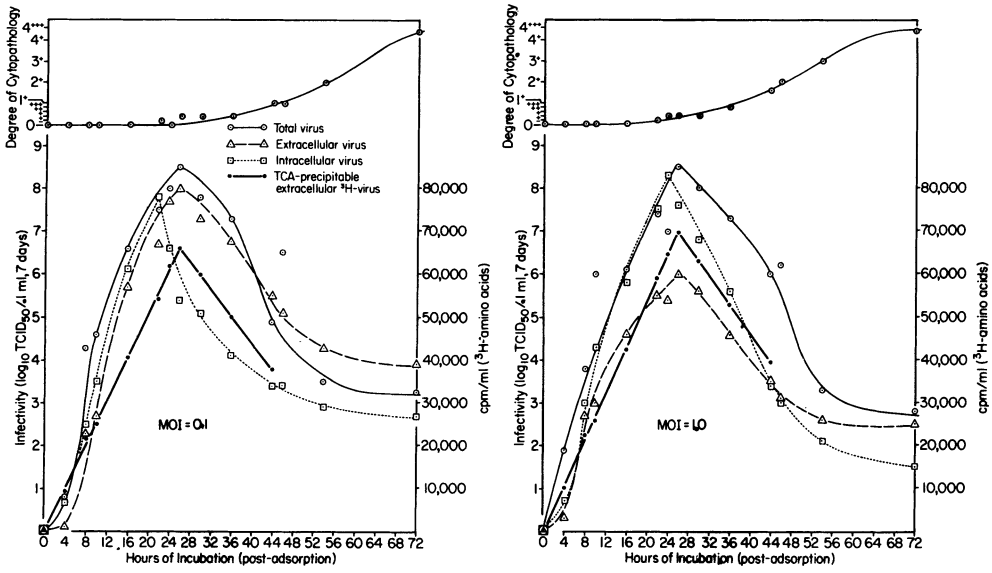

Fig. 1. Growth curves of 229E in HELF cells at MOI = 0.1 & 1. Peak titers of infectious intracellular virus at 22-24 hr were followed by peak titers of infectious extracellular and total virus and by peak levels of ^{3}H-labeled virus at 26 hr postadsorption, when CPE was minimal. Maximum CPE was coincident with rapid autolysis of the virus as it remained at 35°C. CPE was scaled from + (5% of cells visibly affected) to +++ (20%) to 1^{+} (25%) to 4^{+} (100%) to 4^{+++} (all cells totally destroyed).

that 229E contains five amino acids in concentrations of >8 mol%: aspartic acid, glutamic acid, leucine, serine, and valine. Possibly it is the additional requirement for one or more of these amino acids which results in increased virus yield in fortified cultures.[40]

Similar infectious virus results were obtained by Macnaughton et al., who found highest infectivity titers of 229E in MRC fibroblasts 32 hr after infection.[41] In their study, discrete foci of virus were found by indirect immunofluorescence as early as 8 hr after infection, and numbers of foci were correlated with increasing infectivity titers.

Strain 229E is a relatively poor test antigen and a weak immunogen. The IHA and CF antigen titers are considerably lower than one would expect from nine logs of virus, and the IHA, CF, and SN titers (1:80, 1:128, 1:40, respectively) of antiserum to purified virions also are much lower than expected. Although Bradburne reported two precipitin lines in ID tests between 229E and human 229E-convalescent sera,[23] we consistently found only one line in both ID and IE tests with convalescent human sera and with rabbit antiserum versus 10-log preparations of crude or purified virus.[40]

Virus synthesized under optimum conditions of growth was purified for analysis of constituent proteins by PAGE. Two purification schemes were used: (1) the procedure described for OC-43 utilizing adsorption to and elution from human "O" erythrocytes, followed by dialysis and adsorption to calcium phosphate gel; the gel was sequentially washed with phosphate buffers of 0.001 to 0.2 M, pH 7.2, and the virus eluted with 0.3 M buffer;[30] and (2) precipitation of clarified extracts with PEG-6000 and centrifugation to equilibrium through shallow glycerol/tartrate gradients; the virus band was then recentrifuged through steep glycerol/tartrate equilibrium gradients for 16 hr or rate zonal gradients for 4.5 hr.[40]

Procedure (1) gave a mean 5800-fold reduction in total protein with a 67% yield. Procedure (2) gave a mean 5100-fold reduction in total protein with a 96% yield. Both schemes were approximately equal in their removal of host cell proteins, with the final products containing <0.02% of crude tissue culture proteins and <0.007% of crude culture radioactivity. The criteria of purity established for OC-43 were met for 229E as well.

Absorption spectra of different lots of purified 229E at weighed concentrations of 1 mg/ml or less revealed a mean maximum at 256 nm and a mean minimum at 241.2 nm. The mean O.D. 260/280 ratio was 1.53; the specific extinction coefficient, $\underline{k}$, for a 1% solution and a 1-cm light path was $51.8_{O.D.260}$ and $34.0_{O.D.280}$; the extinction coefficient, $E^{1\%}_{1cm}$, had a mean value of 54.3 at 256 nm. All values were corrected for light scattering.

Gel electrophoresis was carried out in continuous phosphate gels as used for OC-43[30] and in discontinuous Tris-glycine gels.[40] Gels were stained for protein, phosphoprotein, glycoprotein, and lipoprotein and scanned as before.[30] Seven polypeptides were consistently found, six of which appeared to contain carbohydrate and one lipid (Table 1). None contained phosphate at a level exceeding 0.6% of the virion by weight.

Electropherograms of labeled virus harvested 26-30 hr after adsorption supported both the purity of the 229E preparations and the composition of the virus as determined by gels stained for protein and carbohydrate (Fig. 2). Again, seven polypeptides in proportions similar to those obtained in stained gels were observed, and only VP-47 was not glycosylated.[40] Our results are somewhat different from those of Macnaughton,[42] who found five major proteins, three of which were glycosylated and two of which were associated with the peplomers (Table 1).

Bromelin treatment of purified 229E removed VGP-106 and VGP-17 entirely and appeared to significantly reduce VGP-165 and VLGP-196. Further studies on the glycoproteins of 229E are in progress and are summarized in the last section of this review.

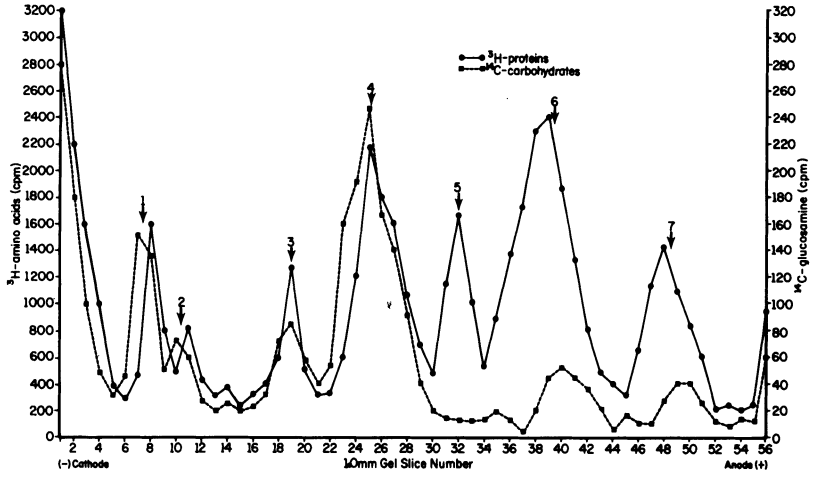

Fig. 2. Radioactive profile of purified 229E virus with ^{3}H-labeled proteins and ^{14}C-labeled carbohydrates. The viral proteins were electrophoresed in 3%/8% gels in the discontinuous Tris buffer system.

Sedimentation coefficients for 229E were measured between 15,000 and 19,000 rpm on Schlieren optics. Uncorrected coefficients averaged 359 x 10^{-13} sec. Values corrected for solvent density and viscosity, for partial specific volume of the virus, and for infinite dilution gave a sedimentation coefficient of $S^{\circ}_{20,w}$ = 381 S. Equilibrium runs with 229E were of limited value due to the rapid disintegration of the virus at 20°C.

RNA OF STRAIN OC-43

The RNA of strain OC-43 was examined by prelabeling 4-day-old suckling mice intracerebrally with approximately 320 µCi of ^{32}P orthophosphate, followed at 8 hr with $10^{4.22}$ LD_{50} of virus by the same route.[43,44] Brains were harvested at 40 hr and virus present was purified by freezing and thawing the suspension 4x, clarifying, and adsorbing to and eluting from human "O" cells. The final eluate was concentrated and centrifuged to equilibrium at 97,100g for 15 hr through a 25-65% sucrose gradient in NET buffer at 7°C. The lower coincident peak of radioactivity, hemagglutinin, and CF activity was then recentrifuged through a 15-65% sucrose velocity gradient for 1 hr at 43,200g. The upper peak of radioactivity and hemagglutinin was used as the starting material for RNA studies. RNA extraction was carried out by five different methods in an effort to find the method best suited for OC-43 RNA.

RNA was prepared from two samples of ^{32}P OC-43 virus by the warm phenol-SDS (WPS) method and from two other samples by the SDS-lysis (SL) method.[45,46] Profiles of OC-43 and marker RNAs from each

gradient after centrifugation are shown in Fig. 3. When the WPS method was used and the RNAs were examined in 15-30% sucrose gradients (Fig. 3A), most RNA was distributed broadly in the 15-50S region of the gradient, with a smaller quantity of 4S RNA also present. Analysis in 5-20% gradients (Fig. 3B) suggested that the

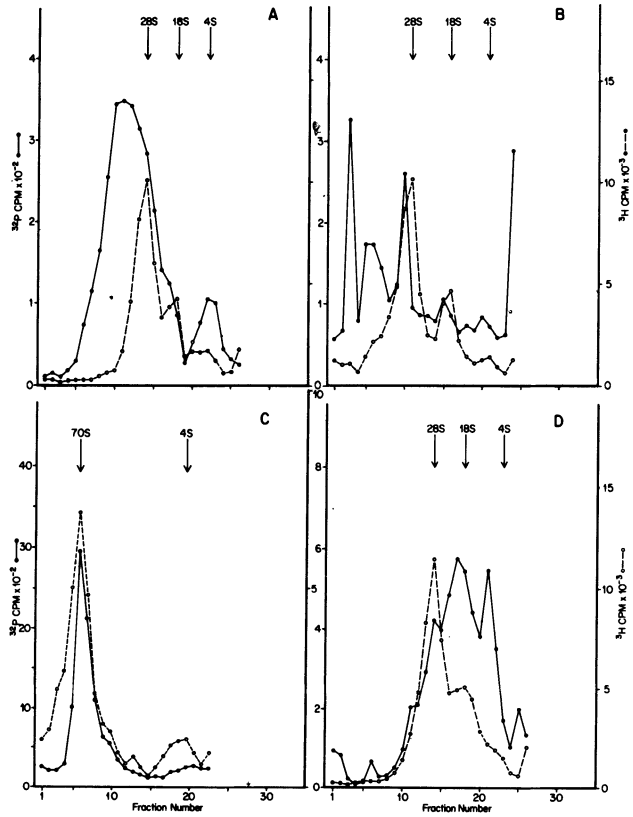

Fig. 3: Sucrose gradient analysis of OC-43 RNA prepared by extraction methods used for other coronaviruses. RNA was extracted from two samples of ^{32}P OC-43 virus by the WPS method (A & B). After extraction, carrier and ^{3}H-uridine ribosomal RNA were added and all RNAs were precipitated with ethanol. Each precipitate was dissolved in 0.5 ml NET and analyzed by ultracentrifugation in 4.4 ml 15-30% (A) or 5-20% (B) sucrose gradients. RNA from two further samples (C & D) was released by the SL method. Sample C was mixed with 0.1 ml of ^{3}H-uridine RSV RNA. Sample D was first mixed with 0.1 ml of ^{3}H-uridine ribosomal RNA and 100 µg carrier RNA, and all RNAs were precipitated with ethanol, resuspended in 0.5 ml NET, and analyzed by centrifuging through 15-30% sucrose gradients. The profiles of acid-insoluble radioactivity, fractionated onto paper strips, are shown for OC-43 (—●—)and ribosomal or RSV (--O--) RNA.

RNA was distributed throughout the gradient, and no resolution between the smaller 4S and larger heterogeneous RNA classes was possible. When the SL method was used to release viral RNA (Fig. 3C), a single large homogeneous RNA was obtained with a sedimentation coefficient identical to the major (70S) component of Rous Sarcoma Virus (RSV) RNA. The OC-43 RNA is best described as a 70S RNA on the basis of repeated sucrose gradients cocentrifuged with various RNA markers. When RNA was released by the SL method, precipitated with ethanol, and reconstituted in NET (Fig. 3D), a smaller and more heterogeneous range of RNA species was obtained, suggesting a breakdown of the large RNA noted in Fig. 3C.[43]

In view of differences in the RNA profile for OC-43 noted in Fig. 3, RNA profiles were obtained by the SDS-pronase (SP), phenol-chloroform (PC), and perchlorate-chloroform-isoamyl alcohol (PCIA) extraction methods.[43,47,48] By the SP method, a more homogeneous major RNA component with a sedimentation coefficient of 45-50S and a minor 4S component were apparent (Fig. 4A). Extraction by the PC method (Fig. 4B) revealed a heterogeneity in the RNA fragments comprising the major class similar to that noted with the WPS method (Fig. 3A); a minor 4S component also was present. Complete RNA degradation occurred after extraction by the PCIA method, indicating its unsuitability for OC-43 RNA extraction (Fig. 4C). Degradation is probably caused by an interaction between outer virion components oxidized by perchlorate treatment and virion RNA, similar to that described for periodate treatment of myxoviruses. The PC

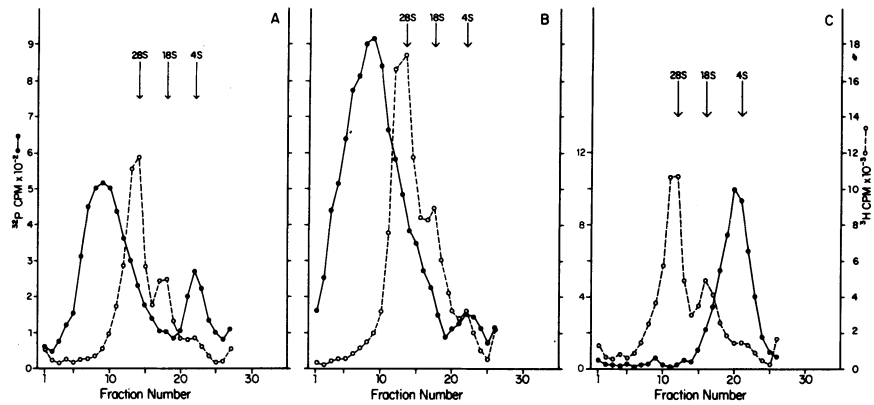

Fig. 4: RNA profiles for OC-43 virus obtained by other extraction procedures. ^{32}P OC-43 RNA was extracted by the (A) SP, (B) PC, and (C) PCIA procedures. Each extract was combined with 0.1 ml ^{3}H-uridine ribosomal and 100 µg of carrier RNA and precipitated with ethanol. The precipitates were resuspended in 0.5 ml NET and analyzed in 15-30% sucrose gradients. The distributions of acid-insoluble radioactivity are shown for OC-43 (—●—) and ribosomal (--0--) RNAs.

method was used for all subsequent extractions involving phenol because of the greater RNA yields obtained and the observation that phenol-chloroform mixtures conserved polyadenosine sequences in RNA.[43]

The profile obtained for OC-43 RNA by sucrose-gradient centrifugation was compared with one obtained by PAGE. The RNA typically migrated as a homogeneous complex with an electrophoretic mobility similar to that of 45S ribosomal precursor RNA. Acrylamide gels electrophoresed at 23°C revealed considerable breakdown of the complex; this thermolability of OC-43 RNA was confirmed in later experiments. The electrophoretic profiles of OC-43 RNA, after preparation by the PC and SP methods, were then determined at 5°C. Clearly, the PC method resulted in considerable breakdown of the large complex into a range of RNA fragments with electrophoretic mobilities between 45S and 18S (Fig. 5A). A minor 4S component was also present; it was similar to that found for IBV RNA after extraction by the WPS method.[45] RNA prepared by the gentler SP method was more homogeneous (Fig. 5B), but some degradation, evidenced by apparent trailing of the major peak, and a minor 4S component can still be seen. The latter appears to be released from the major 70S complex by the WPS, PC, and SP methods.

A semilogarithmic plot of molecular weight versus electrophoretic mobility of the data from replicate experiments gave a mean apparent molecular weight of 6.1×10^6 for the undegraded RNA complex. OC-43 RNA, when prepared by the SL method, has an identical electrophoretic mobility to 70S RSV RNA.[43] Because of the complexity of RSV RNA, however, it was not used as a molecular weight marker.

Garwes et al. reported that RNA complexes from the porcine coronaviruses TGEV and HEV were degraded if extracted by SDS lysis at temperatures above 60°,[46] as has been noted for the RNAs of Retroviridae. To confirm this with OC-43 RNA, preparations of OC-43 virus were treated with 1% SDS by the SL method at 23°, 37°, and 60° C. The distributions of acid-insoluble radioactivity for each gradient suggest that some breakdown of the 70S complex into smaller 4S fragments occurred at 37°C and a more generalized breakdown to a range of intermediate species occurred at 60°C. Because little dissociation of the HEV and TGEV RNAs occurred at temperatures less than 60°C,[46] the OC-43 RNA complex seems even more labile than that of the porcine coronaviruses. Additionally, the 4S RNA component obtained by the two phenol extraction methods or the SP method appears to be derived from the larger 70S complex.

Heterogeneity in the major RNA component of OC-43 after phenol extraction (Figs. 3,4,5) may have been caused by (1) mechanical disruption by phenol of noncovalent bonds linking the OC-43 RNA fragments which form the 70S complex or (2) specific release or

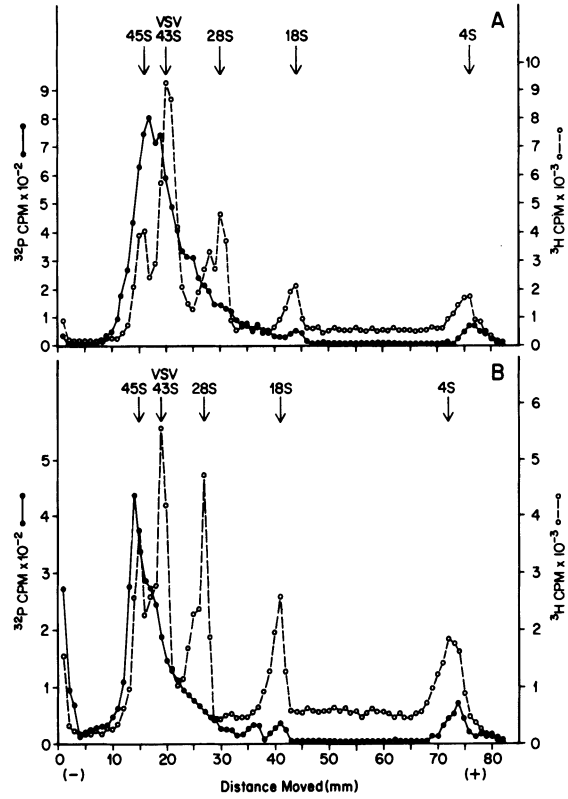

Fig. 5: PAGE of ^{32}P OC-43 RNA extracted by (A) the PC and (B) the SP methods. ^{3}H-uridine ribosomal and ^{3}H-uridine VSV RNA and 50 µg of carrier RNA were added to each, and all RNAs were precipitated with ethanol. The precipitates were dissolved in 100 µl NET; sucrose and bromphenol blue were added to final concentrations of 10% and 0.01%, respectively; and 60 µl aliquots were electrophoresed. The distributions of radioactivity for OC-43 (—●—) and ribosomal and VSV (--0--) RNAs are shown.

activation of virion ribonucleases in the extraction procedure. To examine these possibilities, we coextracted RNAs from mixtures of ^{32}P OC-43 virus and ^{3}H-uridine TMV or ^{3}H-uridine RSV by the PC method. TMV RNA contains a single piece of RNA with a sedimentation coefficient of 31S. The major 70S RNA of RSV is comprised of smaller fragments of variable size and linked by noncovalent bonds; a number of minor RNA components are also present. RNAs in each mixture, after preparation, were precipitated with ethanol in the presence of carrier RNA and analyzed in sucrose gradients. The profiles of acid-insoluble radioactivity for each gradient showed the same heterogeneity for the major class of OC-43 RNA fragments already noted by the phenol extraction method (Figs. 3,4) and

again confirm the presence of a minor 4S component. Both TMV RNA and 70S RSV RNA remained undegraded after extraction, suggesting that the heterogeneity of the major RNA class is caused not by the activation of ribonucleases but by disruption of noncovalent linkages between RNA fragments which are much weaker than similar linkages within the 70S RSV RNA. Sedimentation coefficients for the major RNAs released by phenol (15-55S) were less than the homogeneous 70S peak obtained by the SL method (Fig. 3C).

Further evidence that OC-43 70S RNA is a complex of fragments held together by weak, noncovalent bonds was obtained by (1) isolation of 70S OC-43 RNA by SDS-lysis and centrifugation, followed by PC extraction in the presence of TMV RNA, and (2) isolation of RNA by the SL method and centrifugation in DMSO gradients. OC-43 70S RNA was lysed with SDS and centrifuged to isolate the RNA complex. The profile for total (acid-soluble and -insoluble) radioactivity from aliquots of each gradient fraction revealed a sharp peak of ^{32}P radioactivity in the 70S region (the RNA complex) and a much larger peak of low density material at the top of the gradient. Similarly located but much smaller peaks for acid-insoluble, ribonuclease-resistant radioactivity are seen in Fig. 3C. It, therefore, seems likely that SDS-lysis separates RNA from large amounts of acid-soluble components, some acid-insoluble phospholipids, and perhaps other components in the outer virion coat.

PC extraction in the presence of ^{3}H-uridine TMV RNA followed by ethanol precipitation and analysis in sucrose gradients revealed completely degraded OC-43 70S RNA but intact TMV RNA. This confirms earlier evidence that the 70S complex is held together by weak noncovalent bonds which are destroyed by phenol extraction (Figs. 3,4) or gentle heating. The breakdown of isolated 70S RNA by the PC extraction method is more complete than by similar extraction of purified virions. It does not appear to be due to ribonuclease activity because TMV RNA within the same mixture remains intact.

Since DMSO has been used as a critical test for noncovalent linkages in RSV 70S RNA, we investigated its effect on 70S OC-43 RNA prepared by SDS-lysis. The profile for total radioactivity showed a complete breakdown of the 70S RNA complex to smaller fragments which sediment slightly faster than structural phospholipids at the top of the gradient.

In summary, human coronavirus RNA was characterized using OC-43 virus propagated in suckling mouse brain in the presence of ^{32}P orthophosphate. When isolated from purified virions by SDS-lysis, a single RNA species is obtained which has a sedimentation coefficient of 70S, a molecular weight of 6.1×10^{6}, and is heat-labile. Phenol extraction isolates a range of RNAs with sedimentation coefficients of 15 to 55S, and some 4S RNA is present as

a minor component.[43] We then proceeded to examine OC-43 RNA for the presence of genomic polyadenylic acid (poly (A)) sequences by affinity column chromatography and for the presence of a virion transcriptase with systems optimal for the transcriptases of myxoviruses and paramyxoviruses.[44]

^{32}P-OC-43 RNA was extracted from purified virions by the PC method, precipitated with ethanol in the presence of carrier RNA, and dissolved in NET. Mixtures consisting of OC-43 and a) ^{3}H-uridine poliovirus RNA, b) ^{3}H-uridine VSV RNA, or c) ^{3}H-uridine RSV RNA were applied to poly (U)-Sepharose 4B columns and the filtrates were collected. Nonadherent RNA was removed with washes, and poly (A)-containing RNAs were eluted with a formamide-NET buffer. For each mixture, a significant proportion of OC-43 RNA was removed with the elution buffer, indicating that poly (A) sequences were present. In the controls, significant amounts of poliovirus and RSV RNA (each containing poly (A)) in mixtures (a) and (c) were also eluted, but very little VSV RNA (containing no poly (A)) remained after the washing steps.

The size of the poly (A) residues in OC-43 RNA was determined by sucrose density centrifugation after ribonuclease digestion and passage through a poly (U)-Sepharose 4B column (Fig. 6). The profiles for acid-insoluble radioactivity showed that the poly (A) was present as a single peak with a sedimentation coefficient of 2S located near the top of the gradient. The peak was well resolved from what appeared to be some incompletely digested RNA fragments too large to contain poly (A) alone. The molecular weight of the 2S poly (A) was calculated to be 6645, which corresponds to a stretch of approximately 19 adenylate residues.

Similar profiles were obtained in two further experiments. When pancreatic ribonuclease was omitted from the RNA-enzyme mixture, a larger peak with a sedimentation coefficient of 4S was obtained, indicating that small amounts of nucleotides other than A were present. The polyadenylate 2S fragment represents approximately 0.3% of the total RNA before digestion. The latter figure is a minimal value, however, because larger, incompletely digested, poly (A)-containing fragments were also found (see Fig. 6), which could be due to regions of base pairing within the RNA genome. These may or may not be related to the 2S fragment.

Transcriptase experiments were carried out with systems optimal for influenza and for Newcastle Disease Virus (NDV), along with appropriate controls. For the influenza-type system, transcriptase activity was also measured in mixtures in which i) 2-mercaptoethanol was added, ii) manganous chloride was omitted, and iii) magnesium chloride was omitted. The incorporation obtained for each set of conditions is shown in Fig. 7. For influenza (Fig. 7A), maximum incorporation of 77 pmol UMP/mg virus protein

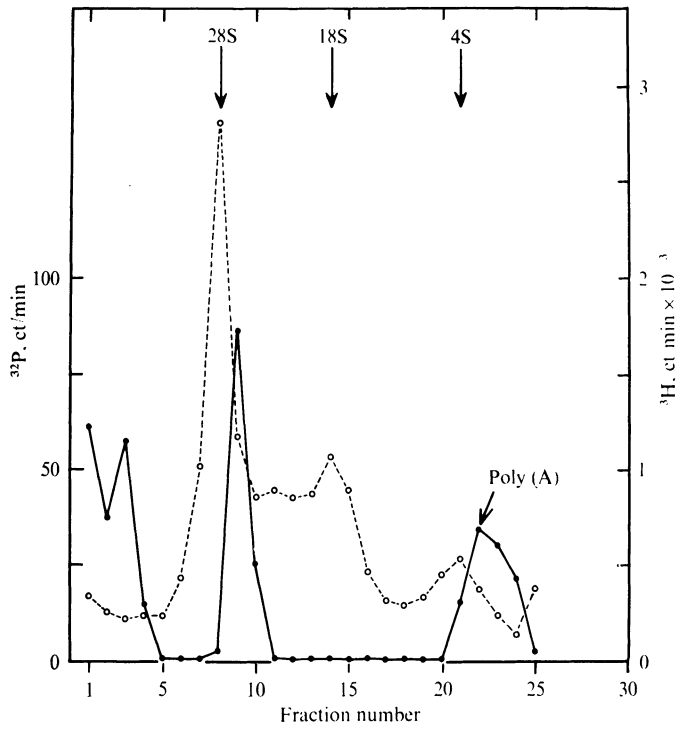

Fig. 6: Sizing of poly (A) sequences in OC-43 RNA. One ml of ^{32}P-OC-43 RNA prepared by PC extraction in NET (0.1 M NaCl, 0.01 M EDTA, 0.01 M Tris, pH 7.4) was incubated with 50 units of ribonuclease T_1 and 10 µg of pancreatic ribonuclease for 60 min at 34°C. The mixture was extracted three times by the PC method and precipitated with ethanol in the presence of carrier RNA. The precipitate was taken up with NET and passed through a poly (U)-Sepharose 4B column. The eluates were further precipitated with ethanol in the presence of carrier and ^{3}H-uridine ribosomal RNA and analyzed in a sucrose-density gradient. The distributions of acid-insoluble, ^{32}P-OC-43 poly (A) (—●—) and ^{3}H-ribosomal RNAs (--O--) are shown.

was obtained after 60 min at 37°C in the standard reaction mixture and in mixtures i and ii. When magnesium chloride was omitted (iii), no incorporation occurred above background. In the same system for OC-43 (Fig. 7B), no incorporation above background occurred under any conditions. With NDV in an NDV-type system (Fig. 7C), incorporation occurred to a maximum of 7 pmol UMP/mg virus protein after 1 hr at 32°C, but no incorporation above background was noted for OC-43 (Fig. 7D). An OC-43 RNA transcriptase was therefore not detected with systems optimal for the transcriptases of morphologically-similar viruses.[44]

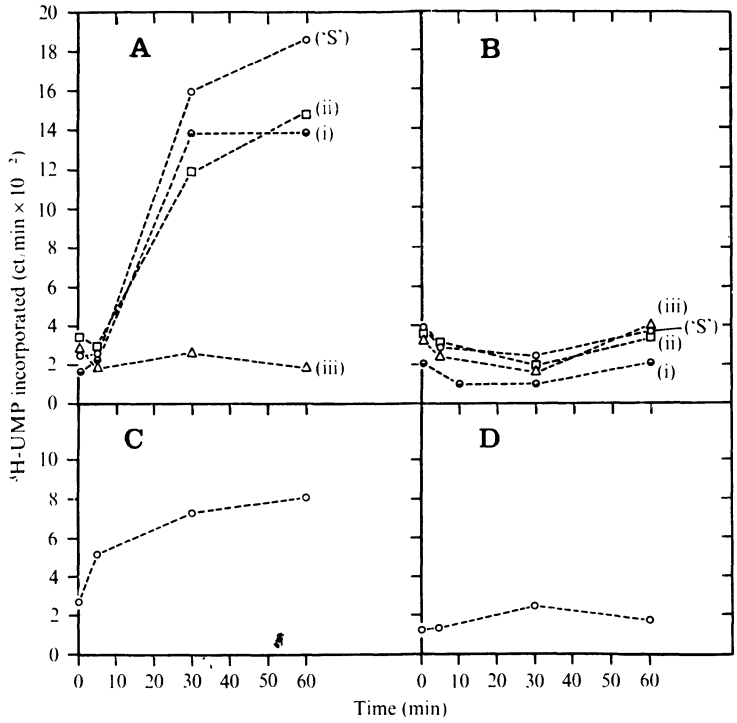

Fig. 7: Tests for the presence of OC-43 virion transcriptase. Transcriptase activity, according to the extent of acid-insoluble ^{3}H-UMP incorporation, was measured for (A) influenza and (B) OC-43, with an influenza-type system, and for NDV (C) and OC-43 (D), with an NDV-type system. For the influenza-type system, besides the standard reaction mixture ('S')additional mixtures were prepared in which (i) 2 µl of 10% 2-mercaptoethanol was added, and (ii) manganous chloride and (iii) magnesium chloride was omitted. The influenza-type system was incubated at 37°C and the NDV-type system at 34°C.

Thus, poly (A) is present in 15-55S OC-43 RNA obtained by PC extraction but absent from the minor 4S RNA, suggesting different functions for each RNA class. A segment of about 19 AMP residues was obtained by T_1 and pancreatic ribonuclease digestion. The function of OC-43 4S RNA in PC extracts is unknown. It may be that the same 4S RNA which is freed from the 70S complex by heating functions as a specific t-RNA, as is the case with retrovirus RNA. Evidence as to whether the poly (A) in OC-43 RNA is internal or is located at the 3' terminus is still incomplete.

RNA OF STRAIN 229E

Studies described above showed that the genome of OC-43 has a molecular weight of approximately 6.1 x 10^6. During ongoing studies of 229E RNA, we attempted to determine the molecular weight of the 229E genome in similar fashion. Virion RNA was labeled with ^{32}Pi and extracted by the phenol-chloroform method. The labeled RNA was then electrophoresed on acid-urea agarose gels with molecular weight markers, and the separated RNA species were visualized by autoradiography.[49] The results showed that the 229E genome has a molecular weight of approximately 6.5 x 10^6. In addition, three other RNA species ranging in size from 16-26S were resolved. Preliminary data indicate that these RNA species are not breakdown fragments of the 70S genomic RNA, but may in fact represent defective interfering RNA molecules.

The estimated size of the 229E genome may be low, since the genome of IBV has been estimated to have a molecular weight of 6.9 x 10^6 by gel electrophoresis and 8.1 x 10^6 by complexity measurements.[50] The size estimate of the 229E genome obtained in our laboratory is somewhat higher than the value of 5.8 x 10^6 reported by Macnaughton & Madge.[51]

In our studies, no replication occurred in the presence of actinomycin-D, even at concentrations of 0.5 μg/ml.[40] However, this and all higher concentrations were toxic for human embryonic lung fibroblasts and, therefore, the inability of the virus to replicate does not necessarily indicate a concomittant requirement for nuclear function. Kennedy & Johnson-Lussenburg found inhibition of replication of 229E with actinomycin D levels as low as 0.1 μg/ml, but this inhibition did not apparently involve viral RNA synthesis.[52] The fact that 229E has a single-stranded RNA[40] and has been shown in ongoing studies to have polyadenylate residues in its genome suggests that its RNA acts as a primary messenger which would obviate the need for a virion transcriptase. Further studies are needed to resolve this question.

BIOSYNTHESIS AND ASSEMBLY OF HUMAN CORONAVIRUSES

Little information has been obtained on the biosynthesis and assembly of OC-43 and 229E. Morphologically, both viruses form by budding into the cisternae of the endoplasmic reticulum between membranes.[53-56] In the earliest stages of development, altered segments of cisternal or reticulum membrane bulging from the cytoplasm into the vesicular lumen were observed in 229E-infected cells.[53] The membrane that seemed destined to become part of the envelope of the virion appeared to be a bilayer. Thus the budding mechanism is not unlike that described for other enveloped viruses that mature at the plasma membrane of infected

cells. The morphogenesis of OC-43 seems to be similar to that of 229E, but discrete steps in the budding process were not observed.[54]

Although direct evidence has not been presented, the dense crescent-shaped structure which forms at the cisternal membrane of 229E-infected cells is probably comprised of a ribonucleoprotein complex (RNP). Such a complex has been isolated from purified virions and shown to consist of a tightly coiled helical or linear nucleocapsid.[57-59] A number of workers agree that the density of the RNP complex is 1.27 g/cm^3, but the reported diameter of the RNP complex ranges from 9-16 nm in width.[57-59] A preliminary analysis of the RNP complex proteins showed that a 45,000-dalton protein was associated with the viral RNA.[57]

The synthesis and assembly of the viral membrane components of a number of enveloped viruses have been studied. First, viral glycoproteins appear to be synthesized on membrane-bound polyribosomes, and glycosylation occurs in association with cytoplasmic membranes. Secondly, glycoproteins appear to migrate from rough endoplasmic reticulum to smooth or Golgi-complex membranes with further modification of viral glycoprotein oligosaccharides. Thirdly, the glycoproteins are inserted into the plasma membrane of virus-infected cells and assembled into virions.[60-62] This pathway has been clearly demonstrated for well characterized members of the myxo- and rhabdovirus groups. But coronaviruses, as described above, do not bud from the plasma membrane of infected cells. Instead, the virions bud into the vesicular lumen and egress from the cell by lysis of the cell or by rupture of virion-containing vesicles at the plasma membrane.[54,56] In fact, the presence of human coronavirus glycoproteins on the surface of the cellular plasma membrane has not yet been demonstrated. Thus, we sought to determine if coronavirus glycoproteins contain glycosyl sidechains similar to those of Sindbis,[63-65] influenza,[66-68] and rhabdovirus virions.[69,70]

To answer this question, coronavirus 229E glycoproteins labeled with ^{3}H-glucosamine were purified and the protein constituents were solubilized and separated by SDS-PAGE as previously described.[71,72] After electrophoresis, the glycoproteins were visualized by fluorography[72] and gel segments corresponding to VLGP-196 (or simply "gp190") were excised and prepared for glycopeptide analysis.[71,72] The gp190 glycopeptides of 229E were co-chromatographed on a Bio-Gel P6 column with ^{14}C-glucosamine-labeled glycopeptides of influenza A/WSN virus.[66] The elution profile of the gp190 oligosaccharide moieties is shown in Fig. 8. The major size class of glycopeptides found corresponded in size to the 2900-dalton influenza glycopeptides.

The 2900-dalton influenza glycopeptides are designated type I and contain glucosamine, mannose, galactose, and fucose.[66]

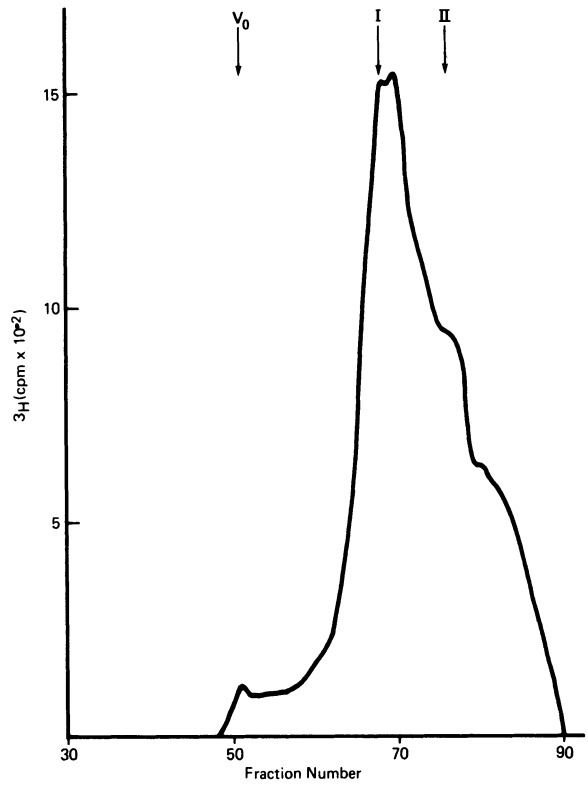

Fig. 8: Analysis of ^3H-glucosamine-labeled gp190 glycopeptides of 229E by Bio-Gel P6 gel filtration. ^{14}C-glucosamine-labeled glycopeptides of influenza A/WSN grown in MDBK cells were co-chromatographed as internal molecular weight markers. The elution positions of the type I glycopeptides (MW = 2900) and smaller type II glycopeptides (MW = 2200) are indicated by solid arrows; V_o = the void volume.

Thus, the major glycopeptide constituent of gp190 appears to contain glycopeptides similar to those of viruses which bud from the plasma membrane.[63-72] Therefore, even though coronaviruses are assembled at sites within the endoplasmic reticulum, the mechanism of synthesis and glycosylation of strain 229E glycoproteins does not appear to differ from that of other well-studied, enveloped viruses.

REFERENCES

1. D. A. J. Tyrrell, J. D. Almeida, D. M. Berry, C. H. Cunningham, D. Hamre, M. S. Hofstad, L. Mallucci, and K. McIntosh, Coronaviruses, Nature 220:650 (1968).
2. A. F. Bradburne and D. A. J. Tyrrell, Coronaviruses of man, Progr. Med. Virol. 13:373 (1971).
3. J. C. Hierholzer, J. R. Broderson, and F. A. Murphy, New strain of mouse hepatitis virus as the cause of lethal enteritis in infant mice, Inf. Imm. 24:508 (1979).
4. K. McIntosh, Coronaviruses: A comparative review, Current Topics in Microbiol. Immunol. 63:85 (1974).
5. A. S. Monto, Coronaviruses, Yale J. Biol. Med. 47:234 (1974).
6. J. A. Robb and C. W. Bond, Coronaviridae, Comprehensive Virology 14:193 (1979).
7. D. A. J. Tyrrell, D. J. Alexander, J. D. Almeida, C. H. Cunningham, B. C. Easterday, D. J. Garwes, J. C. Hierholzer, A. Kapikian, M. R. Macnaughton, and K. McIntosh, Coronaviridae: Second report, Intervirology 10:321 (1978).
8. H. W. Ackermann, G. Cherchel, J. P. Valet, J. Matte, S. Moorjani, and R. Higgins. Experiences sur la nature de particules trouvées dans der cas d'hepatite virale: type coronavirus, antigène Australia et particules de Dane, Can. J. Microbiol. 20:193 (1974).
9. K. Apostolov, P. Spasić, and N. Bojanić, Evidence of a viral etiology in endemic (Balkan) nephropathy, Lancet 2:1271 (1975).
10. J. S. Burks, B. L. DeVald, L. D. Jankovsky, and J. C. Gerdes, Two coronaviruses isolated from central nervous system tissue of two multiple sclerosis patients, Science 209:933 (1980).
11. E. O. Caul and S. K. R. Clarke, Coronavirus propagated from patient with non-bacterial gastroenteritis, Lancet 2:953 (1975).
12. E. O. Caul and S. I. Egglestone, Further studies on human enteric coronaviruses. Arch. Virol. 54:107 (1977).
13. E. O. Caul, W. K. Paver, and S. K. R. Clarke, Coronavirus particles in faeces from patients with gastroenteritis, Lancet 1:1192 (1975).
14. L. Georgescu, P. Diosi, I. Butiu, L. Plavosin, and G. Herzog, Porcine coronavirus antibodies in endemic (Balkan) nephropathy, Lancet 1:163 (1978).
15. A. W. Holmes, F. Deinhardt, W. Harris, F. Ball, and G. Cline, Coronaviruses and viral hepatitis, J. Clin. Invest. 49:45a (1970).
16. M. Mathan and V. I. Mathan, Coronaviruses and tropical sprue in southern India, in: Fourth Int. Cong. for Virol., The Hague, Behring Inst., Frankfurt Germany (1978).
17. R. D. Schnagl, I. H. Holmes, and E. M. Mackay-Scollay, Coronavirus-like particles in aboriginals and nonaboriginals in western Australia, Med. J. Australia 1:307 (1978).

18. A. J. Zuckerman, P. E. Taylor, and J. D. Almeida, Presence of particles other than the Australia-SH antigen in a case of chronic active hepatitis with cirrhosis, Brit. Med. J. 1:262 (1970).
19. D. A. J. Tyrrell and M. L. Bynoe, Cultivation of a novel type of common-cold virus in organ cultures, Brit. Med. J. 1:1467 (1965).
20. D. Hamre and J. J. Procknow, A new virus isolated from the human respiratory tract, Proc. Soc. Exp. Biol. Med. 121:190 (1966).
21. K. McIntosh, J. H. Dees, W. B. Becker, A. Z. Kapikian, and R. M. Chanock, Recovery in tracheal organ cultures of novel viruses from patients with respiratory disease, Proc. Nat. Acad. Sci. 57:933 (1967).
22. A. Z. Kapikian, H. D. James, S. J. Kelly, and A. L. Vaughn, Detection of coronavirus strain 692 by immune electron microscopy, Inf. Imm. 7:111 (1973).
23. A. F. Bradburne, Antigenic relationships amongst coronaviruses, Arch. Gesamte Virusforsch. 31:352 (1970).
24. K. McIntosh, A. Z. Kapikian, K. A. Hardison, J. W. Hartley, and R. M. Chanock, Antigenic relationships among the coronaviruses of man and between human and animal coronaviruses, J. Immun. 102:1109 (1969).
25. K. McIntosh, J. McQuillin, S. E. Reed, and P. S. Gardner, Diagnosis of human coronavirus infection by immunofluorescence: Method and application to respiratory disease in hospitalized children, J. Med. Virol. 2:341 (1978).
26. A. S. Monto and L. M. Rhodes, Detection of coronavirus infection of man by immunofluorescence, Proc. Soc. Exp. Biol. Med. 155:143 (1977).
27. J. C. Hierholzer and G. A. Tannock, Quantitation of antibody to non-hemagglutinating viruses by single radial hemolysis: Serological test for human coronaviruses, J. Clin. Microbiol. 5:613 (1977).
28. H. Riski, T. Hovi, P. Väänänen, and K. Penttinen, Antibodies to human coronavirus OC 43 measured by radial haemolysis in gel, Scand. J. Inf. Dis. 9:75 (1977).
29. H. S. Kaye and W. R. Dowdle, Some characteristics of hemagglutination of certain strains of "IBV-like" virus, J. Inf. Dis. 120:576 (1969).
30. J. C. Hierholzer, E. L. Palmer, S. G. Whitfield, H. S. Kaye, and W. R. Dowdle, Protein composition of coronavirus OC 43, Virology 48:516 (1972).
31. H. S. Kaye, J. C. Hierholzer, and W. R. Dowdle, Purification and further characterization of an "IBV-like" virus (coronavirus), Proc. Soc. Exp. Biol. Med. 135:457 (1970).
32. J. Pokorny, M. Bruckova, and M. Ryc, Biophysical properties of coronavirus strain OC-43, Acta Virol. 19:137 (1975).
33. G. Gerna, E. Cattaneo, P. M. Cereda, M. G. Revelo, and G. Achilli, Human coronavirus OC-43 serum inhibitor and neutralizing antibody by a new plaque-reduction assay, Proc. Soc. Exp. Biol. Med. 163:360 (1980).

34. A. Z. Kapikian, H. D. James, S. J. Kelly, L. M. King, A. L. Vaughn, and R. M. Chanock, Hemadsorption by coronavirus strain OC-43, Proc. Soc. Exp. Biol. Med. 139:179 (1972).
35. T. Hovi, H. Kainulainen, B. Ziola, and A. Salmi, OC 43 strain-related coronavirus antibodies in different age groups, J. Med. Virol. 3:313 (1979).
36. G. Gerna, G. Achilli, E. Cattaneo, and P. Cereda, Determination of coronavirus 229E antibody by an immune-adherence hemagglutination method, J. Med. Virol. 2:215 (1978).
37. H. S. Kaye, S. B. Ong, and W. R. Dowdle, Detection of coronavirus 229E antibody by indirect hemagglutination, Appl. Microbiol. 24:703 (1972).
38. C. A. Kraaijeveld, M. H. Madge, and M. R. Macnaughton, Enzyme-linked immunosorbent assay for coronaviruses HCV 229E and MHV 3, J. Gen. Virol. 49:83 (1980).
39. A. V. Sheboldov, L. Y. Zakstelskaya, and V. M. Zhdanov, Sedimentation and density characteristics of coronavirus, Vopr. Virusol. 1:59 (1973).
40. J. C. Hierholzer, Purification and biophysical properties of human coronavirus 229E, Virology 75:155 (1976).
41. M. R. Macnaughton, B. J. Thomas, H. A. Davies, and S. Patterson, Infectivity of human strain 229E, J.Clin.Micr. 12:462 (1980).
42. M. R. Macnaughton, The polypeptides of human and mouse coronaviruses, Arch. Virol. 63:75 (1980).
43. G. A. Tannock, and J. C. Hierholzer, The RNA of human coronavirus OC-43, Virology 78:500 (1977).
44. G. A. Tannock, and J. C. Hierholzer, Presence of genomic polyadenylate and absence of detectable virion transcriptase in human coronavirus OC-43, J. Gen. Virol. 39:29 (1978).
45. G. A. Tannock, The nucleic acid of infectious bronchitis virus, Arch. Gesamte Virusforsch. 43:259 (1973).
46. D. J. Garwes, D. H. Pocock, and T. M. Wijaszka, Identification of heat-dissociable RNA complexes in two porcine coronaviruses, Nature 257:508 (1975).
47. M. W. Pons, Influenza virus messenger ribonucleoprotein, Virology 67:209 (1975).
48. M. Adesnik, and J. E. Darnell, Biogenesis and characterization of histone messenger RNA in HeLa cells, J. Mol. Biol. 67: 397 (1972).
49. B. P. Holloway, and J. F. Obijeski, Rabies virus-induced RNA synthesis in BHK-21 cells, J. Gen. Virol. 49:181 (1980).
50. D. F. Stern, and S. I. T. Kennedy, Coronavirus multiplication strategy. I. Identification and characterization of virus-specified RNA, J. Virol. 34:665 (1980).
51. M. R. Macnaughton, and M. H. Madge, The genome of human coronavirus strain 229E, J. Gen. Virol. 39:497 (1978).
52. D. A. Kennedy, and C. M. Johnson-Lussenburg, Inhibition of coronavirus 229E replication by actinomycin D, J. Virol. 29:401 (1978).
53. W. B. Becker, K. McIntosh, J. H. Dees, and R. M. Chanock,

Morphogenesis of avian infectious bronchitis virus and a related human virus (strain 229E), J. Virol. 1:1019 (1967).
54. R. A. Bucknall, A. R. Kalica, and R. M. Chanock, Intracellular development and mechanism of hemadsorption of a human coronavirus, OC43, Proc. Soc. Exp. Biol. Med. 139:811 (1972).
55. H. A. Davies, and M. R. Macnaughton, Comparison of the morphology of three coronaviruses, Archives of Virology 59:25 (1979).
56. L. S. Oshiro, J. H. Schieble, and E. H. Lennette, Electron microscopic studies of coronavirus, J. Gen. Virol. 12:161 (1971).
57. E. O. Caul, C. R. Ashley, M. Ferguson, and S. I. Egglestone, Preliminary studies on the isolation of coronavirus 229E nucleocapsids, FEMS Microbiol. Letters 5:101 (1979).
58. D. A. Kennedy, and C. M. Johnson-Lussenburg, Isolation and morphology of the internal component of human coronavirus strain 229E, Intervirology 6:197 (1976).
59. M. R. Macnaughton, H. A. Davies, and M. V. Nermut, Ribonucleoprotein-like structures from coronavirus particles, J. Gen. Virol. 39:545 (1978).
60. J. Lenard, and R. W. Compans, The membrane structure of lipid-containing viruses, Biochem. Biophys. Acta 344:51 (1974).
61. R. W. Compans, and M. C. Kemp, Membrane glycoproteins of enveloped viruses, in: "Current Topics in Membranes and Transport" (R. L. Juliano and A. Rothstein, eds.), Vol. 11, Academic Press, New York, (1978).
62. R. W. Compans, and H. -D. Klenk, Viral membranes, in: "Comprehensive Virology," (H. Fraenkel-Conrat and R. R. Wagner, eds.), Vol. 13, Plenum Press, New York (1979).
63. B. W. Burge, and J. H. Strauss, Glycopeptides of the membrane glycoprotein of Sindbis virus, J. Mol. Biol. 47:449 (1970).
64. B. Sefton, and K. Keegstra, Glycoproteins of Sindbis virus: Preliminary characterization of the oligosaccharides, J. Virol. 14:522 (1974).
65. K. Keegstra, B. Sefton, and D. Burke, Sindbis virus glycoproteins: Effect of the host cell on the oligosaccharides, J. Virol. 16:613 (1975).
66. K. Nakamura, and R. W. Compans, Glycopeptide components of influenza viral glycoproteins, Virology 86:432 (1978).
67. K. Nakamura, and R. W. Compans, Biosynthesis of the oligosaccharides of influenza viral glycoproteins, Virology 93:31 (1979).
68. R. T. Schwarz, M. F. G. Schmidt, U. Anwer, and H. -D. Klenk, Carbohydrates of influenza virus. I. Glycopeptides derived from viral glycoproteins after labeling with radioactive sugars, J. Virol. 23:217 (1977).
69. S. A. Moyer, J. M. Tsang, P. H. Atkinson and D. F. Summers, Oligosaccharide moieties of the glycoprotein of vesicular stomatitis virus, J. Virol. 18:167 (1976).

70. J. R. Etchison, J. S. Robertson, and D. F. Summers, Partial structural analysis of the oligosaccharide moieties of the vesicular stomatitis glycoprotein by sequential chemical and enzymatic degradation, Virology 78:375 (1977).
71. M. C. Kemp, S. Basak, and R. W. Compans, Glycopeptides of murine leukemia viruses. I. Comparison of two ecotropic viruses. J. Virol. 31:1 (1979).
72. M. C. Kemp, N. G. Famulari, P. V. O'Donnell, and R. W. Compans, Glycopeptides of murine leukemia viruses. II. Comparison of xenotropic and dual-tropic viruses, J. Virol. 34:154 (1980).